communications earth & environment

Article

A Nature Portfolio journal

https://doi.org/10.1038/s43247-025-02809-w

Fragmented deoxyribonucleic acid could be extractable from Mars's surface rocks

Maria-Paz Zorzano [1] ✉, Jyothi Basapathi Raghavendra[2], Daniel Carrizo [1], Fuencisla Cañadas [1], Mariana Reyes-Prieto [3], Giuseppe D'Auria [3] & Javier Martin-Torres[2,4]

Detecting biomolecules in rocks is vital for understanding life's evolution on Earth and its possible existence on Mars. The *Curiosity* rover measured Total Organic Carbon (TOC) levels of 201–273 ppm in 3500 million years (Ma)-old Martian mudstones exposed to radiation for 78 ± 30 Ma. Here we investigate whether deoxyribonucleic acid (DNA), a unique biological polymer, can be recovered under comparable conditions. We extracted and sequenced DNA from terrestrial sedimentary rocks with TOC ranging from 182 to 63,000 ppm, yielding 184,000 to 3.8 million nucleobases from a 0.5 g rock sample. After exposure to 10.45 MGy of gamma radiation, equivalent to 136 Ma on the Martian surface, we measured a radiolytic constant of $K = 0.17\ MGy^{-1}$ in microbialite (2800-year-old) and oxide iron formation (2930 Ma old) samples. Despite fragmentation, 1.48–8.45% of sequences remained taxonomically identifiable, demonstrating that DNA fragments can persist in rocks for over 100 Ma.

The study of organic molecules preserved in ancient sedimentary rocks can provide insights into the evolution of life on Earth and its potential existence on Mars. The earliest widely accepted evidence of life on Earth includes microbial mats, preserved as stromatolites, dating back to 3500 million years (Ma) [In this text, we use "Gy" to refer to radiation units. To prevent confusion between time and radiation units, we use "a" to represent years instead of "y" following standard notation. As a result, "Ma" stands for million years] formed in shallow marine environments[1,2]. During this period, Mars also hosted liquid water, suggesting potential habitability[3]. This raises the possibility that life may have emerged on Earth and Mars during the same period of time.

In situ analysis by the *Curiosity* rover at Gale Crater, Mars, indicates that a shallow lacustrine environment existed around 3600 Ma, supporting habitability conditions[3]. The Sample Analysis at Mars (SAM) instrument measured Total Organic Carbon (TOC) concentrations of 201–273 ppm in 3500 Ma-old lacustrine mudstones from Yellowknife Bay[4]. Following their initial deposition, these mudstones experienced rapid burial, which helped preserve their organic content. Subsequent erosion removed the overlying material, exposing the rocks to cosmic radiation for approximately 78 ± 30 Ma[5]. Various simple organic molecules have been identified in situ at Gale Crater[4,6–11], suggesting the idea that ancient Martian environments may have had conditions suitable for prebiotic chemistry and the preservation of organic compounds. Notably, the most recent findings from the SAM instrument report the detection of long-chain alkanes (C_{10} to C_{12}) in the Cumberland mudstone, representing the largest organic molecules identified on the Martian surface to date and demonstrating the potential for long-term preservation of more complex organics despite the ~3.7 Ga age of the mudstone and ~80 Ma of cosmic ray exposure[12].

These findings strengthen the scientific justification for sample return missions, such as the NASA/ESA Mars Sample Return (MSR)[13] and China's Tianwen-3 mission[14], and for future in situ robotic or crewed missions focused on the search for life. The first part of the MSR mission is already underway with the *Perseverance* rover, which has been exploring Jezero Crater: an ancient paleolake system that once supported fluvial and lacustrine environments conducive to prebiotic chemistry and, perhaps, life[15,16]. The crater's deltaic deposits, formed by episodic water inflow at ~3700–3800 Ma, consist primarily of fine-grained mudstones, sandstones, and conglomerates, suggesting prolonged aqueous activity and past habitability[17,18]. Since 2021, *Perseverance* has been systematically sampling these geologically diverse regions, collecting sealed rock cores (3–7 cm in length, 13 mm in diameter, and weighing ~10–25 g)[15,19–21]. In situ analyses by the *Perseverance* rover at Jezero Crater have provided strong evidence for the presence of organic compounds within Martian rocks. SHERLOC data revealed that these organics are closely associated with sulfate and carbonate minerals[22], suggesting mineralogical contexts favorable to preservation. Supporting this, Scheller et al. (2022)[23] reported that organics co-occur with hydrated phases formed during aqueous alteration, highlighting the potential for past habitable conditions. While fluorescence signals offer key detection pathways, some may arise from inorganic sources, underscoring the complexity of spectral interpretation[24]. Together, these findings

[1]Centro de Astrobiología (CAB), CSIC-INTA, Madrid, Spain. [2]Department of Planetary Sciences, School of Geosciences, University of Aberdeen, Aberdeen, Scotland. [3]Sequencing and Bioinformatics Service, Foundation for the Promotion of Health and Biomedical Research of the Valencian Community (FISABIO), Valencia, Spain. [4]Instituto Andaluz de Ciencias de la Tierra (IACT), CSIC, Granada, Spain. ✉e-mail: zorzanomm@cab.inta-csic.es

emphasize the importance of mineral-organic interactions in assessing biosignature preservation on Mars. After being brought to Earth, Martian samples will undergo analysis in a biosafety-controlled laboratory to search for biosignatures while maintaining containment until the samples can be deemed safe for release by the planetary protection safety assessment protocol[25]. This objective emphasizes the importance of examining biomolecules, at concentrations as low as parts per billion (ppb), and even lower, as potential evidence of past or present life.

DNA (deoxyribonucleic acid) is the most definitive biomolecule for life, as is universally used by all known terrestrial cellular life forms, i.e., prokaryotes (bacteria and archaea) and eukaryotes (plants, animals, fungi and protists). DNA uniquely encodes genetic information, forming the foundation of genetic inheritance. Its identification as a biosignature is uncontroversial because no non-biological processes are known to produce it. DNA is a long polymer made up of repeating units called nucleotides. Each nucleotide consists of three components: a phosphate group, a deoxyribose sugar molecule, and a nucleobase. The recent analysis of the samples returned from asteroid *Bennu* by NASA's OSIRIS-REx mission has identified all the nucleobases found in terrestrial DNA and RNA (ribonucleic acid) within the asteroid regolith samples, which contain roughly 4wt% carbon. Although there is no evidence for polymers of nucleobases with sugar and phosphate group, each gram of *Bennu* sample contained an average of 101 ng (101×10^{-9}g) of uracil (U), 71.973 ng of thymine (T), 34 ng of cytosine (C), 67 ng of adenosine (A), and 18 ng of guanine (G)[26]. This asteroid is estimated to be about 4500 Ma old.

The detection of nucleobases in *Bennu*, at levels of several parts per billion (ppb = 10^{-9}), suggests that the fundamental building blocks of DNA can form and persist in extraterrestrial environments over geological timescales. Research on carbonaceous chondrites, such as the *Murchison* and *Orgueil* meteorites, and the *Ryugu* asteroid (see Extended Data Table 6 in ref. 26), has also shown the presence of extraterrestrial nucleobases, supporting the idea that prebiotic chemistry may have also occurred beyond Earth. However, what remains uncertain is whether nucleotide polymers (rather than just individual nucleobases) could have formed on Mars during its habitable period and, if life did arise, whether DNA polymers could survive over time when exposed to cosmic radiation. Understanding the long-term preservation of DNA in geological substrates over multimillion-year timescales is critical for Mars exploration, particularly for life detection and biosafety assessments.

DNA remains the principal marker for life detection due to its biological specificity and established role in identifying terrestrial contamination. However, synthetic biology has expanded the landscape of genetic polymers to include Xeno Nucleic Acids (XNAs), a class of nucleic acid analogues with non-natural backbones or sugar moieties that still support heredity and molecular recognition[27]. Among the known XNAs are Threose Nucleic Acid (TNA), Glycol Nucleic Acid (GNA), and Peptide Nucleic Acid (PNA): 1) TNA uses a four-carbon sugar (threose) and shows potential for prebiotic evolution[28]; 2) GNA employs a minimal glycol backbone and exhibits high thermal and chemical stability[29]; and 3) PNA, which replaces the sugar-phosphate backbone with a neutral peptide-like scaffold, offers exceptional resistance to enzymatic and hydrolytic degradation[30]. These and other XNAs demonstrate that alternative genetic systems are chemically viable and could, in principle, serve as information carriers in extraterrestrial environments. However, given their shared reliance on base-pairing and polymeric stability for heredity, it is reasonable to expect that their response to ionizing radiation would parallel that of DNA, particularly in terms of strand breakage, base damage, and secondary structure disruption. Therefore, DNA remains an appropriate and informative model for investigating radiation-induced damage in potential nucleic acid–based life beyond Earth.

The oldest DNA recovered on Earth, dating back approximately 2 Ma, was extracted from organic-rich sediments in northern Greenland[31]. Previously, the oldest known preserved DNA came from three mammoth specimens from the Early and Middle Pleistocene, two of which are over 1 Ma old[32]. On Earth, heat accelerates DNA degradation by causing the loss of functional groups and reducing the average molecular weight[33], while biological activity further breaks down organic compounds. Ancient DNA fragments are quickly reduced to 40–500 base pairs (bp) and develop lesions due to depurination and cytosine deamination[34]. The primary environmental factors driving organic degradation include microbial activity, hydrolysis, oxidation, pH, temperature fluctuations, and sedimentary processes. Microorganisms degrade organics through enzymatic reactions, while water promotes hydrolysis, accelerating molecular breakdown. Additionally, oxygen-rich environments enhance oxidation, and extreme pH or temperature shifts destabilize complex biomolecules. Over geological timescales, the pressure from burial and diagenesis further alter organic materials, affecting their preservation.

However, these factors are largely irrelevant on present-day Mars, where plate tectonics, active volcanism, and liquid water are absent, and the only ongoing resurfacing process is minimal aeolian erosion. Today, Mars is hyperarid and cold[35,36], conditions that favor organic preservation but are inhospitable to life as we know it. The scarcity of liquid water limits hydrolytic breakdown, while Mars's thin atmosphere reduces the role of atmospheric oxygen in organic degradation. However, Mars's surface contains highly reactive oxidants, including perchlorates (~ 0.4–1 wt%), as detected by *Phoenix* and *Curiosity*[37,38], and also highly reactive oxygen-containing species such as superoxide ions, peroxides, and hydroxyl radicals, which can form through UV photolysis, radiolysis, and mineral-mediated redox reactions[39–41]. These reactive species can potentially degrade organics. Additionally, with no global magnetic field and only a tenuous atmosphere, the Martian surface is exposed to intense cosmic and solar radiation, making radiation-induced degradation one of the most significant challenges for the long-term preservation of organic matter[42,43]. Interestingly, recent studies suggest that over 95% of uracil and 92% of purine nucleobases added at 25–50 ppm to a 5 cm thick Martian mudstone analogue (kaolinite) rock, can withstand a dose of 0.072 MGy[44]. This suggests a radiolytic constant of $K = 1.11$ MGy^{-1} (for purine) and 0.73 MGy^{-1} (for uracil), supporting the possibility of nucleobases to survive radiation exposure embedded within Martian rocks.

The *Perseverance* rover sample collection consists of igneous and sedimentary rocks, rich in silica and iron oxides, with carbonates, and chloride and sulfate salts. Future Mars missions targeting past habitable environments (and potential biomarker preservation) will likely focus on similar rock types. In this study, we examine terrestrial analogue rocks from carbonate- and iron-rich sedimentary environments, in saline aqueous settings, that have undergone different degrees of diagenetic and metamorphic transformation. The goal of this research is to evaluate the potential of these sedimentary rocks to preserve DNA after exposure to radiation levels equivalent to 100 million years on the Martian surface.

Results

Sample collection and preparation

We assembled a collection of analogue sedimentary rocks, including 2800-year-old microbialites (see Fig. 1A), 541 Ma-old stromatolite (see Fig. 1B), and carbonate (see Fig. 1C, D) and oxide iron formation samples from Earth's oldest carbonate sedimentary platform (2930 Ma). Further details on the geological origins of these samples are provided in the Materials and Methods section.

The samples were pulverized and sealed in borosilicate glass vials, replacing the air in the headspace with nitrogen (N_2), see Fig. 2A. A set of sealed samples was exposed to sterilization-level gamma irradiation doses of 1) $D_1 = 0.86$ MGy (see Supplementary Fig. 1) and geological-timescale doses of 2) $D_2 = 10.45$ MGy (see Fig. 2B–D). To reduce DNA contamination in the laboratory analysis, all extractions, dilutions, and library preparations for sequencing were conducted in an ISO (International Organization for Standardization) Level 5 cleanroom[45], see Fig. 2E. The sample preparation and analysis workflow are illustrated in Fig. 2 and described in detail in the Material and Methods section.

Ultra-low biomass detection limit

All sample types were analysed by nanopore sequencing in triplicate, see Table 1 and Supplementary Tables 1 and 2. To assess potential kitome

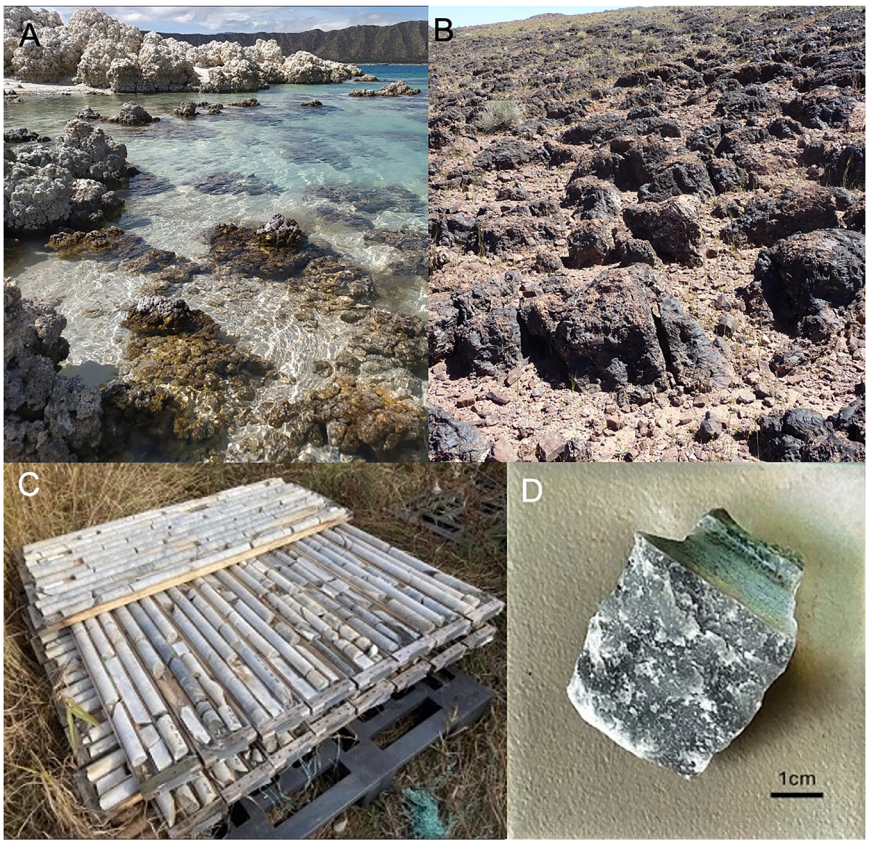

Fig. 1 | Analogue sedimentary sample collection. A A microbialite (~ 2800-year-old) was sampled in Alchichica, Mexico, an alkaline crater lake with high concentrations of NaCl and Na_2CO_3. These microbialites formed through microbially mediated carbonate precipitation and remain submerged in shallow waters, where they continue to accrete carbonate minerals and support diverse microbial communities. **B** A stromatolite (~ 541 Ma) was sampled from this field in Morocco, which is part of the Mançour Group within the Ouarzazate Supergroup (Anti-Atlas region). This carbonate stromatolite formation (400 m × 500 m) developed in a shallow marine environment and was later buried beneath volcanic and volcaniclastic sediments. Tectonic uplift and erosion during the late Paleozoic and Cenozoic exposed the stromatolites, which are primarily composed of limestone ($CaCO_3$) and dolomite ($CaMg(CO_3)_2$), formed by cyanobacteria-driven sediment trapping and binding before the Cambrian explosion. **C** Carbonate samples (~ 2930 Ma) from drilled cores extracted from a depth of 133 m, in the carbonate formation from the Bridget Lake area. These samples consist of dolomite ($CaMg(CO_3)_2$). They precipitated in an open marine environment as dissolved calcium and bicarbonate ions reached saturation. Cyanobacteria likely influenced this process through photosynthesis, which removed CO_2, increased carbonate alkalinity, and promoted mineral precipitation. **D** Detailed view of a carbonate formation fragment (~ 2930 Ma). Small portions (4–5 g) were extracted from fragments of each sample type for further analysis.

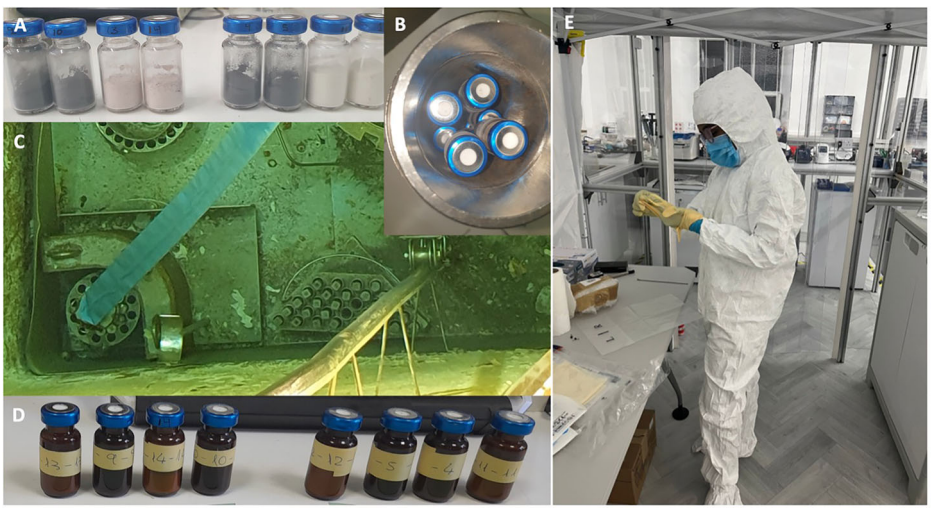

Fig. 2 | Sample preparation and analysis workflow. A Sample sealing under N_2 atmosphere: About 4–5 g of pulverized rock samples were sealed in vials under a neutral, dry atmosphere (N_2 gas). **B** Hermetic container preparation: half of the samples were placed inside a container, which was then hermetically sealed with a lid. **C** Gamma irradiation exposure: The container was submerged in the irradiation facility pool, surrounded by Co^{60} units, and exposed to radiation. The net radiation rate inside the container was 21.91 kGy/h, the total accumulated dose on the sample after 20 days was D_2 = 10.45 MGy. **D** Radiation-induced changes: The irradiated sample vials show a color change in the borosilicate glass after radiation exposure. **E** DNA extraction and sequencing of irradiated rocks: samples were removed from the vials and processed in the ISO 5 cleanroom, where DNA extraction and sequencing were conducted.

Table 1 | Characterization of DNA threads from pristine and gamma irradiated rock samples (D_1 = 0.86 MGy and D_2 = 10.45 MGy) across various rock formation ages and composition, compared to a blank sample of nuclease-free water

3 replicates (0.5 g)	T ±σ_T	L ± σ_L	GC ±σ_GC	Q± σ_Q	K (MGy^{-1})	TOC (ppm) ±σ_TOC
Blank	153,239 ± 122,063	63 ± 10.47	41.33 ± 5.13	3.13 ± 0.23	-	-
Microbialite (~2800 a)	3,813,449 ± 1,392,360	659.23 ± 362.37	59 ± 1.73	8.5 ± 0.85	-	63,262.30 ± 9230.3
Microbialites (~2800 a), 0.86 MGy	1,403,205 ± 835,166	169.53 ± 41.75	48.33 ± 4.73	4.97 ± 0.67	1.161 ± 0.585	18,870.40 ± 3951.4
Microbialites (~2800 a), 10.45 MGy	665,510 ± 247,034	189.33 ± 64.77	44.33 ± 3.79	3.9 ± 0.75	0.168 ± 0.085	42,841.36 ± 17,660.5
Stromatolites (~541 Ma)	748,005 ± 500,367	216 ± 65.76	45.67 ± 2.52	4.33 ± 0.71	-	448.79 ± 213.7
Stromatolites (~541 Ma), 10.45 MGy	917,383 ± 427,995	210.5 ± 43.59	49.67 ± 2.52	3.87 ± 0.72	-	182.75 ± 16.4
Oxide iron formation (~2930 Ma)	1,097,511 ± 370,325	199.33 ± 76.46	44.33 ± 1.15	3.63 ± 0.21	-	8500 ± 1000[46]
Oxide iron formation (~2930 Ma), 10.45 MGy	184,893 ± 15,993	150.37 ± 40.06	44 ± 5.00	3.57 ± 0.25	0.171 ± 0.080	-
Carbonate (~2930 Ma)	760,257 ± 475,632	140.03 ± 54.24	44 ± 1.00	3.57 ± 0.60	-	619.68 ± 304

Average and standard deviation of total amount of bases T, mean length L (in number of bases), mean GC % content — i.e., the percentage of number of guanine (G) and cytosine (C) bases relative to the total number of sequenced bases, calculated as (G + C) / T × 100 —, and mean quality factor Q over three replicates. The radiolytic constant K after exposure to a dose D, is calculated comparing the total number of bases before and after irradiation. TOC was analysed independently from three to four replicates of the same sample type.
DNA was extracted from 0.5 g of rock per replicate.

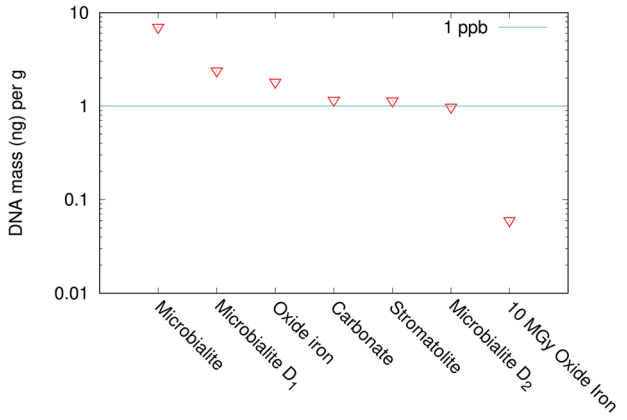

Fig. 3 | Sequenced DNA mass (in ng) per gram of sample, a reference limit set at 1 ppb is included for comparison. After exposure to 10.45 MGy of radiation, the oxide iron formation, which is primarily composed of magnetite ($Fe^{2+}Fe^{3+}{}_2O_4$) and chert (SiO_2), exhibits the lowest DNA yield of 0.05 ng per gram. In addition to this, the kitome contamination adds about 0.13 ng per analysis.

contamination, three control samples (blank) were processed with the same DNA extraction and library preparation kits using nuclease-free water. The total organic carbon (TOC) content of the rocks was also measured for three or four replicates (see Supplementary Table 3), for all samples, except for the oxide iron formation sample, whose TOC was previously determined[46].

In pristine samples there is a linear correlation between the total number of sequenced bases (T) from sequenced DNA extracted from rock samples and the total organic carbon (TOC), as shown in Supplementary Fig. 2 (left). Additionally, a linear relationship exists between the total number of bases and the DNA mass measured by Qubit fluorometry in microbialite samples, as illustrated in Supplementary Fig. 2 (right). In non-irradiated microbialite, the DNA mass was $M_0 = 3.81 \pm 0.27$ ng per 0.5 g of sample, while in the irradiated microbialite (D1), it decreased to $M = 1.77 \pm 0.59$ ng per 0.5 g of sample. In all other cases, the DNA mass was below the detection threshold of the Qubit fluorometer. A linear regression analysis reveals that this method detects approximately 1.046×10^6 bases (i.e. 1 Mb) per nanogram of DNA extracted from rock samples, as shown in Supplementary Fig. 2 (right). Using this linear relationship as a calibration curve, and after subtracting the blank, we can estimate the mass of DNA (ng) per 1 g of rock, as presented in Fig. 3. It is important to note that the DNA extracted and sequenced in this study derives from contemporary microbial communities inhabiting an ancient rock matrix (up to ~2.93 Ga) and, thus, represents modern genetic material. Ancient subsurface rocks can support metabolically active modern microorganisms, as demonstrated in recently recovered 2.0 Ga mafic rock cores, where living microbial populations were identified[47].

It should be noted that nanopore sequencing is also applicable to RNA, although this requires distinct extraction protocols and quantification methods. While RNA possesses biomarker potential, its significantly lower chemical stability and generally shorter polymer length compared to DNA limit its practical use. Consequently, we have focused on DNA owing to its greater molecular stability, longer polymer length even after exposure to radiation, and the availability of comprehensive reference databases, which collectively enhance the reliability of microbiome analyses in rock samples.

Radiation impact

The radiolytic constant of nucleobases was calculated for the microbialite and iron sample cases using the equation $T = T_0 \exp(-K \cdot D)$, where T and T_0 represent the final and initial total number of bases, respectively, after exposure to a radiation dose D (see Table 1 and Fig. 4). The radiolytic degradation constants (K) determined following exposure to a dose of $D_2 = 10.45$ MGy are highly similar for both the iron oxide formation ($K = 0.171 \pm 0.080$ MGy^{-1}) and the microbialite sample ($K = 0.168 \pm 0.085$ MGy^{-1}). When the two datasets are combined, the resulting radiolytic constant is $K = 0.17 \pm 0.09$ MGy^{-1}, suggesting consistent degradation behaviour across these lithologies. In contrast, in the stromatolite sample, the number of nucleotides across the three replicates showed considerable variability both before and after irradiation (see Supplementary Information Table 1), with no discernible reduction in the mean value T. This may suggest that the stromatolite rock is more effective in shielding against radiation, or that the microbiome within the stromatolite is highly dispersed and faint, leading to inconsistent values in each replicate.

All analysed DNA samples exhibit highly fragmented reads (see Table 1 and Figs. 5 and 6). The read length histograms show different distributions based on sample type (see Fig. 6). All rock DNA samples have a few reads that are 50,000–100,000 bp or longer whereas blank sample reads are shorter (Supplementary Fig. 3). The median read length of the Microbialite (~2800 a) is 304 bp, whereas after exposure to 10.45 MGy is 47 bp. The median read length of the oxide iron formation (~2930 Ma) is 57 bp, whereas after exposure to 10.45 MGy, it is 46 bp (see Supplementary Information Table 2).

Taxonomic classification of the microbiome

Despite the damage induced by radiation, the irradiated DNA reads can be sequenced successfully, with signals surpassing that of kitome contamination (blank). The quality score Q decreases significantly for sequences shorter than 600 bp. In metagenomic analysis, short DNA sequences with low Q scores are usually discarded. However, even degraded nucleobase fragments from damaged and fragmented DNA in rocks contain information, and can serve as biomarkers, allowing, in the case of terrestrial samples, to do phylogenetic investigations. Between 1.48 and 51.94% of the sequences matched existing databases of terrestrial organisms, offering insights into the rock's microbiome (see Supplementary Table 2). For the irradiated samples, despite fragmentation, 1.48–8.45% of sequences remained taxonomically identifiable. We performed the genus-level taxonomic tree analysis concatenating the reads of the 3 replicates and subtracting the blank taxonomy (See Figs. 7 and 8 and Supplementary Figs. 4 and 5).

Discussion

This study introduces a novel approach using nanopore sequencing to analyse DNA extracted from just 0.5 g of rock, with yields as low as 0.6 ng (D_2 irradiated microbialite, stromatolite and carbonate) to 3.10 ng of DNA mass (microbialite). The analysis of DNA is performed with nanopore technology, without amplification, enabling the direct quantification of nucleobases and the characterization of read length distributions. This method has been applied here to investigate DNA preservation in rocks exposed to gamma radiation. With NASA/ESA's Mars Sample Return[13] and China's Tianwen-3 returned sample missions[14] on the horizon, discussions about in situ life searching robotic missions and human exploration accelerating, there is an urgent need for a transformative yet feasible approach to life detection. Due to its sensitivity, this approach holds potential for biosafety assessments, contamination control, and life detection in returned Martian samples, as well as for the reconstruction of microbiomes in terrestrial rocks. In particular, this methodology shows strong potential as a payload for future in situ robotic missions to Mars and other potentially habitable extraterrestrial environments, enabling biosignature detection and planetary biosafety assessment.

The cleanroom analysis of irradiated stromatolite samples (~ 541 Ma), which contain only 183 ppm of organic carbon and approximately 0.65 ng of DNA in a 0.5 g rock sample (i.e. 1.3 ppb), shows that nanopore sequencing can generate around 0.9 Mb of DNA fragments without the need for amplification. It is worth noting that the total organic carbon content (TOC) of this rock is similar to that reported for the mudstones at Gale Crater on Mars. Despite radiation exposure, fragmented DNA can still be sequenced and phylogenetically assigned, offering insights into the rock's microbiome. In the DNA extracted from terrestrial sedimentary rocks, we observe a linear correlation between the total amount of nucleobases and the total organic content of the rock, see Supplementary Fig. 2-(Left). This correlation in the four pristine (non-irradiated) rock samples suggests that, in these rocks, endolithic microbial life is at least partially sustained by preserved organic matter and thus that rocks are organic carbon-limited oligotrophic environments. It also suggests that the microbiome of the rocks has a critical role in the decomposition, transformation, and recycling of organic carbon. A strong microbial biomass–TOC correlation reinforces the idea that organic-carbon-rich sites are prime candidates for life detection efforts.

Recent studies employing the Qiagen DNeasy PowerSoil Pro DNA extraction kit on Mars-analog soils have reported comparable DNA yields across diverse extreme environments[48]. This research has shown DNA concentrations ranging from ~0.9 ng/g in Antarctic Dry Valley soils, a hyperarid, cold desert, to ~100 ng/g in calcium carbonate deposits formed by ancient hydrothermal activity in the Trona Pinnacles (California), in an arid, desert region[48]. These findings align with expectations for such low-biomass environments, where extreme desiccation and temperature

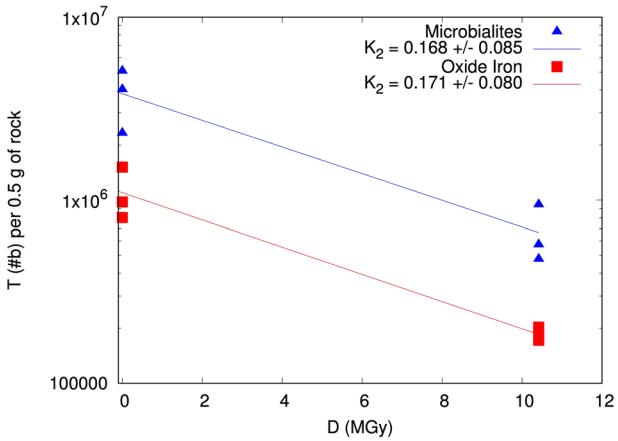

Fig. 4 | Calculation of the nucleobase radiolytic constant K = 0.17 ± 0.09, after exposure to D_2 = 10.45 MGy of gamma radiation. An exponential fit is applied to the triplicate measurements of microbialite and oxide iron formation samples, before and after irradiation. Despite differences in the nature, age, and environment of these sedimentary rocks, the observed DNA radiolytic decay is similar.

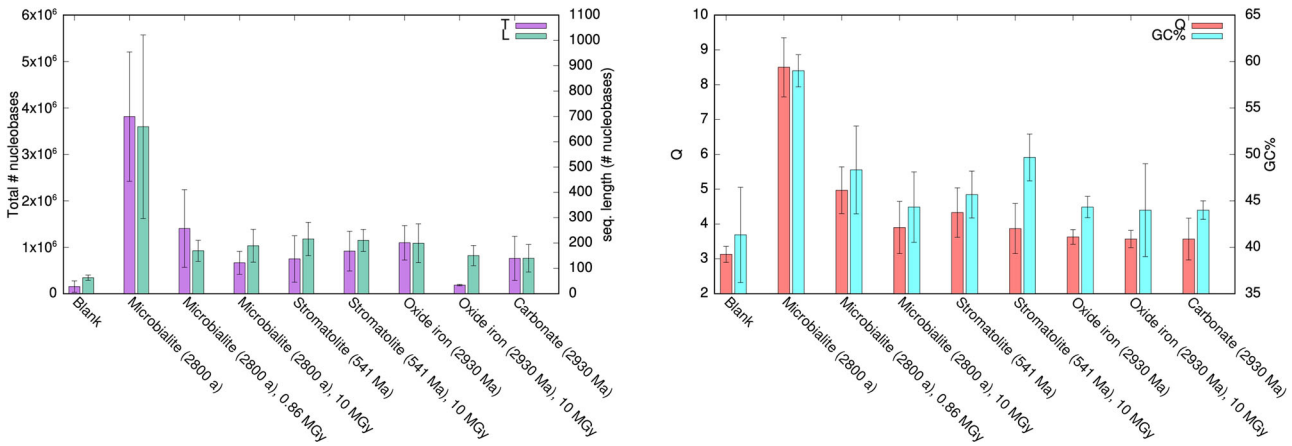

Fig. 5 | Radiation induces a significant reduction in the total mean amount of nucleobases and in the mean fragment length in the microbialite and oxide iron formation cases. Mean and standard deviation of (left) the total nucleobase content (T) and sequence length (L), and (right) the quality factor (Q) and GC% content for all samples and the blank. In the microbialite and oxide iron formation samples, radiation exposure clearly causes DNA fragmentation and nucleobase destruction. In the microbialite samples, radiation exposure clearly reduces Q and GC%.

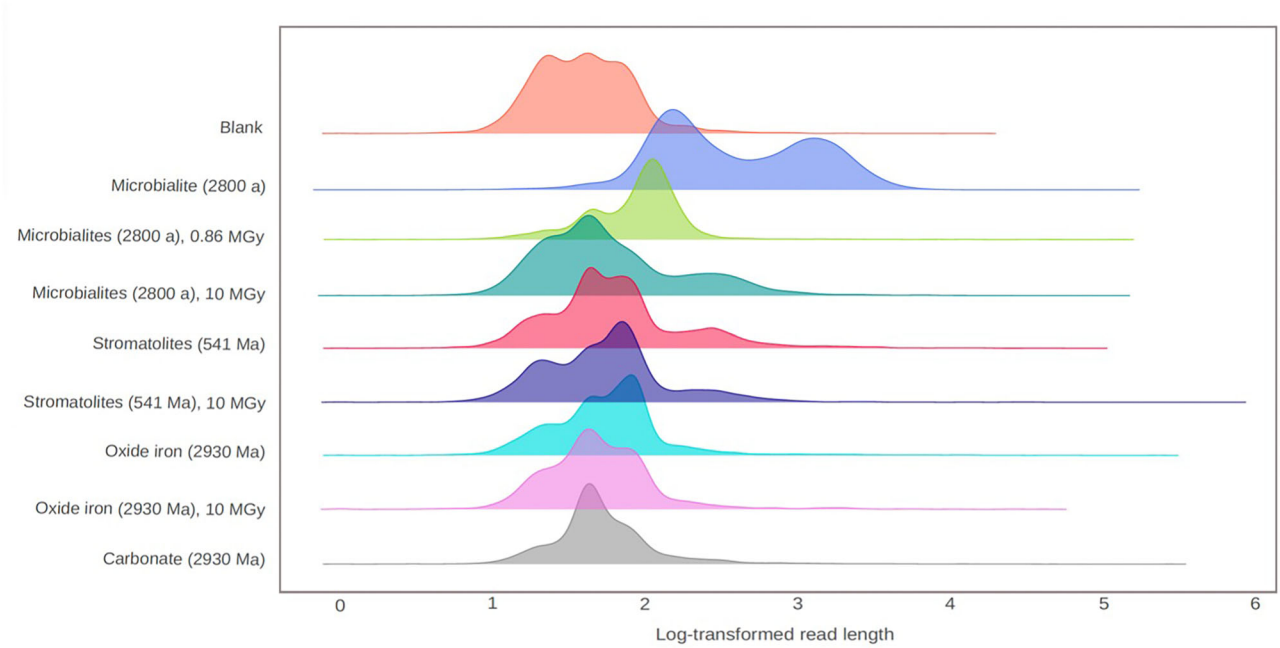

Fig. 6 | Normalized histogram distribution of sequenced DNA reads as a function of nucleobase length (log-transformed). The distribution of DNA read lengths shifts toward shorter reads after radiation exposure, with this effect being most pronounced in the microbialite and oxide iron formation samples. In all other samples, DNA fragments were very short. The median read length of the microbialite (2800 a) is 304 bp, whereas after exposure to 10.45 MGy, it is 47 bp. The median read length of the oxide iron formation (~2930 Ma) is 57 bp, whereas after exposure to 10.45 MGy, it is 46 bp, see Supplementary Information Table 2.

fluctuations significantly limit microbial survival and reproduction. Importantly, this work demonstrated that DNA recovery efficiency can vary by up to a factor of 50, depending on the extraction method, even within the same soil type. In our study with rocks, and Qiagen DNeasy PowerSoil Pro DNA extraction kit, we have observed DNA yields ranging from 0.03 to 6 ng/g in pulverized rock samples, falling within the expected range for ultra-low biomass settings.

The presence of salts, particularly perchlorate salts, present at 0.5–1 wt% in Martian regolith[49], pose significant challenges for DNA preservation and sequencing. As strong oxidizers, perchlorates can degrade nucleic acids, especially under UV exposure, complicating extraction and detection efforts[50]. High salt concentrations also disrupt nanopore sequencing by altering ionic conductivity, increasing noise, and occasionally blocking nanopores[51,52]. To address this, desalting and purification protocols are essential for maintaining DNA integrity in salt-rich samples[53]. Similar approaches should be applied to future Martian samples containing salts.

A critical consideration in such studies is the contribution of kitome DNA contamination, which persists even under stringent decontamination protocols. Our analysis, conducted under ISO 5 cleanroom conditions, indicates that reagents DNA contamination can contribute up to ~0.13 ng per sequencing dataset. These findings highlight the necessity of rigorous contamination control strategies and methodological refinements to enhance the reliability of DNA-based biosignature detection in planetary exploration and astrobiology.

Further research is needed to optimize DNA extraction methods for ultra-low biomass environments and to develop bioinformatics approaches capable of distinguishing indigenous microbial signals from extraneous contamination. The use of blanks is crucial in this process. For example, in this work the taxonomic classification identified human contamination (*Homo sapiens*) in the blank, as well as in samples of carbonate, iron oxide formation, stromatolite, and stromatolite D1-irradiated samples. Consequently, *Homo sapiens* sequences were subtracted in the phylogenetic tree analysis of the studied samples.

As for the future analyses of samples returned from Mars, contamination could lead to false positives when assessing Martian rock samples for polymers of nucleotides, potentially complicating the identification of biosignatures. To mitigate this risk, martian samples could be analysed in a Biosafety Level 4 (BSL-4) facility, which operates under the highest planetary protection standards[13,25]. All equipment, reagents, and instruments used in this facility must undergo rigorous decontamination protocols to ensure the complete absence of exogenous DNA. Additionally, continuous ambient monitoring and strict quality control measures should be implemented to document and quantify background DNA contamination (including reagents), ensuring the integrity of life-detection experiments. Previous studies on laboratory cleanliness, such as those conducted on the OSIRIS-Rex with the *Bennu* asteroid samples[26], underscore the necessity of stringent protocols to prevent terrestrial contamination in astrobiological investigations of extra terrestrial samples. Similarly, before its flight to Mars, the *Perseverance* rover's sampling tubes and drills were assembled on Earth under strict contamination control, including thorough cleaning and the use of flight witness tubes[54]. The Hayabusa and Hayabusa2 missions implemented strict contamination control measures, including sterilization of sampling mechanisms and the use of witness plates to monitor and document terrestrial contamination during sample collection and return[55,56].

In both the microbialite and oxide iron formation samples, exposure to $D_2 = 10.45$ MGy resulted in a radiolytic constant of $K = 0.17$ MGy^{-1} (see Fig. 4). However, no detectable degradation was observed in the stromatolite samples. Notably, these samples exhibited the lowest TOC content. We hypothesize that the high variability in the total number of nucleobases per replicate may be attributed to an uneven and sparse distribution of microorganisms. Alternatively, the stromatolite mineral composition itself may provide enhanced shielding against radiation. For lower dose $D_1 = 0.86$ MGy, we obtain for the microbialite samples, $K = 1.161 \pm 0.585$. This is comparable with the reported $K = 1.11$ MGy^{-1} after exposure to a dose of 0.072 MGy, for purine, added in 25–50 ppm to a 5 cm long kaolinite (mudstone) rock sample[44]. Previous experimental studies suggest that the radiolytic constant of amino acids increases with mass[43]. As for other organic molecules it has been shown that, glutamic acid exhibited a radiolysis constant of 0.172 MGy^{-1} at a similar dose to D_1, while 8-aminoctanoic acid showed no degradation under the same conditions[57]. Other research on

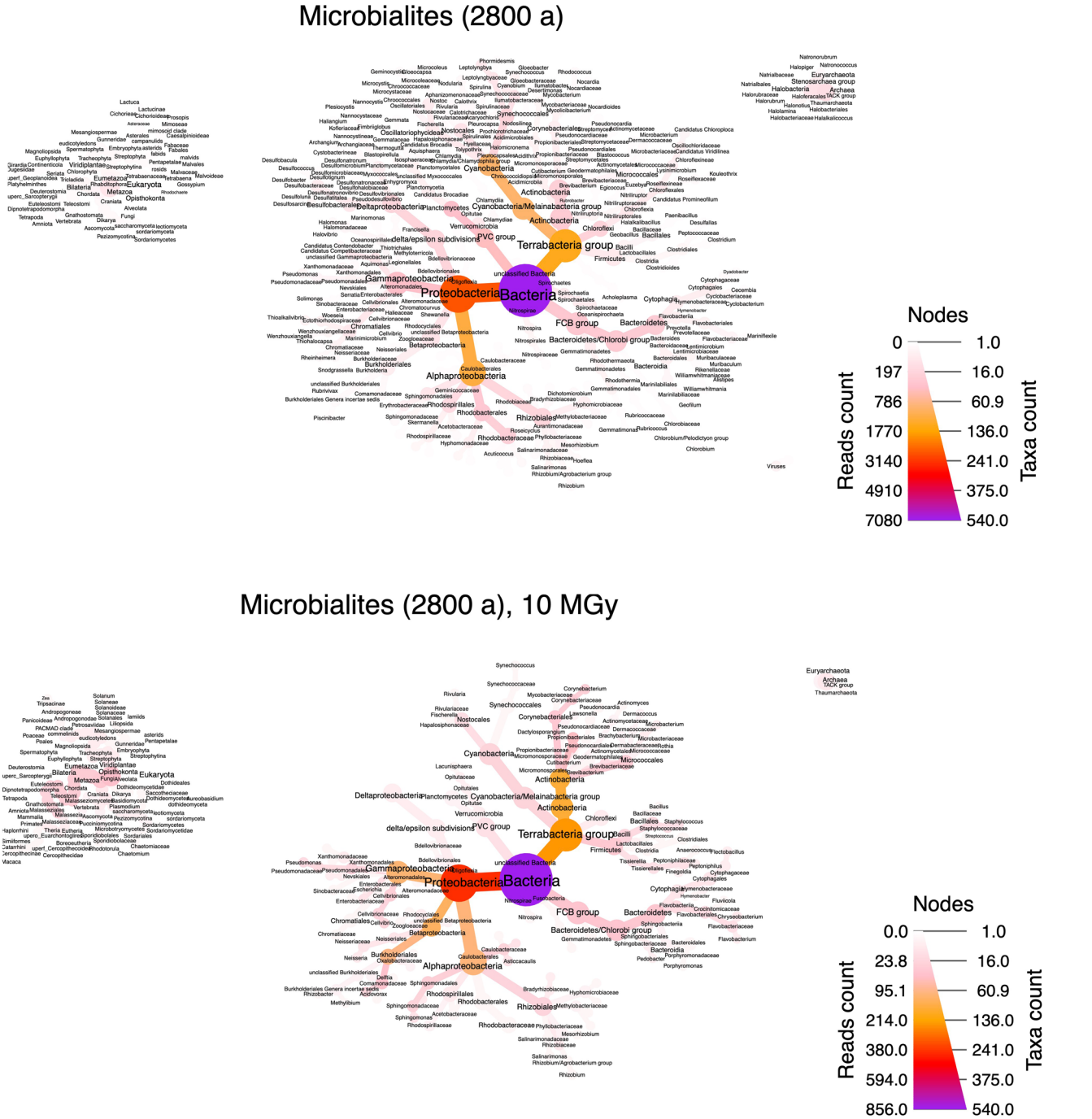

Fig. 7 | Genus-level taxonomic tree constructed from 1.5 g (three replicates) of ~2800-year-old microbialite samples, collected from a shallow, alkaline lake where they remain submerged. The analysis compares microbiome diversity between non-irradiated samples (top) and samples subjected to a radiation dose of 10.45 MGy (bottom), simulating 136 million years of exposure on Mars.

amino acid preservation in silica at liquid nitrogen temperatures and varying radiation doses indicates $K_{glycine}$ (SiO_2 in LN_2) = 0.36 ± 0.04 MGy^{-1} and $K_{isovaline}$ (SiO_2 in LN_2) = 0.45 ± 0.01 MGy^{-1}[58]. The variation in K values across different organic molecules, materials and doses suggests that the mineral matrix and the specific molecular structure of the organics significantly influence the radiation-induced reactivity. Lower values of K indicate that a molecule is more resistant to degradation under radiation, while higher values indicate a greater susceptibility. Our analysis of DNA in rocks, shows that radiation induces nucleobase damage and DNA fragmentation. The median read length of the microbialite (~2800 years) DNA reads before radiation exposure is 304 bp, whereas after exposure to 10.45 MGy is 47 bp. The median read length of the oxide iron formation (~2930 Ma) is 57 bp, whereas after exposure to 10.45 MGy, is 46 bp (see Supplementary Information Table 1). Although DNA exhibits a radiolysis constant comparable to that of other organic molecules, our experiments indicate that its long polymeric structure allows it to undergo radiation-induced fragmentation, yielding smaller segments that often retain informative sequence data.

It is important to note that our irradiation experiments were conducted at near-room temperature (17 °C–19 °C), which is higher than the current estimated maximum temperatures experienced by surface materials on Mars, for instance at Jezero Crater (−20 °C for outcrops and +10 °C for

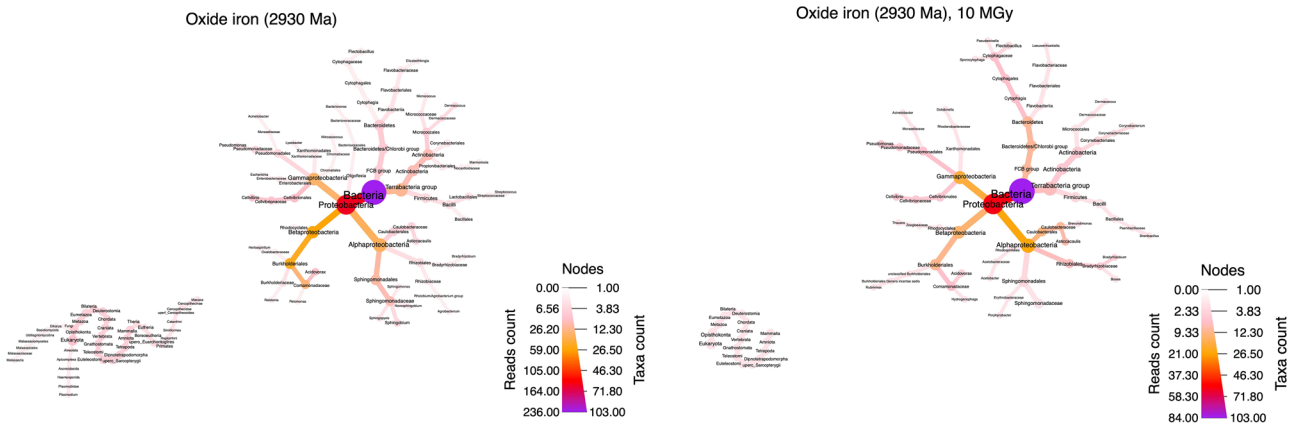

Fig. 8 | Genus-level taxonomic tree derived from 1.5 g (three replicates) of ~2930 Ma-old oxide iron formation samples, collected from a depth of approximately of 67.8 m, within the carbonate platform of the Red Lake area. The analysis compares microbiome diversity between non-irradiated samples (left) and samples exposed to a radiation dose of 10.45 MGy (right), simulating the equivalent of 136 million years of exposure on Mars.

regolith) based on thermal modeling[59]. Previous studies have shown that radiolysis rates can decrease significantly at lower temperatures; for instance, glycine irradiated at −50 °C exhibited a radiolysis rate approximately 1.8 times lower than at room temperature[57]. Conversely, the presence of perchlorates, detected on Mars, may enhance radiolytic degradation, with magnesium perchlorate increasing glycine radiolysis rates by ~1.5 times[57]. These factors suggest that our results may slightly overestimate or underestimate DNA degradation under Martian surface conditions, depending on local temperature and mineralogy.

In situ measurements of the Radiation Assessment Detector (RAD) instrument on Curiosity at Gale crater indicate that the present-day galactic cosmic ray radiation dose on Mars is 0.07665 Gy/year[60]. Extrapolating from these measurements, a dose of 10.45 MGy corresponds to 136 Ma of exposure to radiation on the surface of Mars, which is greater than the exposure time of the mudstones at Gale Crater, where the SAM instrument measurements report a TOC of about 200 ppm. Our analysis shows that rocks may adequately shield nucleobase polymers from radiation for over 100 million years on Mars, facilitating the investigation of extant or recently extinct life. Near-surface sedimentary rocks in Gale Crater exhibit a wide range of cosmic-ray exposure ages, with samples like Cumberland and Windjana showing relatively short exposure times of approximately 78 and 45 Ma, respectively, consistent with scarp retreat erosion processes[5]. However, the Mojave 2 sample displays more complex exposure ages, with ^{3}He measurements suggesting up to ~1 Ga and ^{36}Ar data indicating ~300 Ma, implying that some sedimentary rocks on Mars may have experienced significantly longer cosmic-ray exposure than those tested in this study[61]. The degradation impact of other Martian environmental conditions, like perchlorate exposure or thermal cycling of the rock samples with condensation, hydration, dehydration and sublimation water cycles, should also be explored in the future. These effects may accentuate radiation damage as the interaction of water and salts with radiation produces highly reactive species[62,63].

This study demonstrates that although nucleobases are significantly damaged by radiation and DNA polymers are fragmented, the remaining DNA threads still contain important biological information. Despite considerable degradation, 1.48–8.45% of the remaining DNA fragments were still taxonomically identifiable (see Figs. 7 and 8, and Supplementary Information Table 2). The taxonomic trees illustrate that each sample type possesses a unique phylogenetic signature, confirming that the identified DNA reads are indigenous rather than contaminants. Notably, the analysis of irradiated DNA continues to provide a coherent representation of the rock's microbiome genera.

The phylogenetic tree analysis of both pristine and irradiated microbialite samples reveals the presence of *Cyanobacteria*, a dominant group in microbialite structures (see Fig. 7). Earlier phylogenetic studies on the microbialites of Alchichica lake, utilizing small subunit ribosomal RNA gene sequencing and amplification[64], have identified overlapping bacterial orders, including *Cyanobacteria, Alphaproteobacteria, Betaproteobacteria, Gammaproteobacteria, Deltaproteobacteria, Firmicutes, Actinobacteria, Verrucomicrobia, Planctomycetales, Chloroflexi, Bacteroidetes, Chlorobi, Nitrospirae*, and *Spirochaetes*. Specifically for *Cyanobacteria*, we also identified taxa similar to those previously reported[64], such as *Nostocales* and *Pleurocapsales*. Additionally, our analysis detected eukaryotic groups (*Viridiplantae, Alveolates, Fungi, and Metazoa*) which were also reported[64], but revealed a greater microbial diversity, including *Archaea*.

In the oxide iron formation sample, we identified *Acidovorax, Acinetobacter*, and *Acetobacter*, all of which are iron oxidizers and metal-tolerant microorganisms capable of surviving in acidic environments (see Fig. 8 and Supplementary Table 2). Similarly, the microbiome of the stromatolite and carbonate samples, also shows a distinctive community that can be directly linked to this type of rocks (see Supplementary Figs. 4 and 5, and references herein). The sequenced DNA represents microorganisms that currently inhabit the rock, which may have been introduced through water, diagenetic fluids, or air. Although the microbial diversity information extracted from the extremely ancient rocks represents modern life, this work shows that the microbial record remains largely intact even after the irradiation.

There is consensus in the astrobiology community that any proposed life detection approach requires measurements to be highly sensitive, contamination-free, and repeatable[65]. Any putative biosignature must be detectable, preserved, reliable (distinct from abiotic signals), and compatible with known life forms, with a biological interpretation only made after all possible abiotic hypotheses have been ruled out as suggested in NASA's Confidence of Life Detection (CoLD) scale[66]. There are natural environmental conditions that can result in the abiotic synthesis of nucleobases, however, only life can form long (over several thousand) nucleotide polymers. In our study, all natural and irradiated rock samples, the extracted DNA has at least a few reads that are 50,000 bp or longer. Based on our analysis of the rocks, we propose that a correlation of the total amount of sequenced nucleobases with TOC, combined with the detection of nucleotide polymers of different lengths, especially long reads, may serve as a potent indicator of life in oligotrophic environments such as Mars. Nanopore technology shows potential for sequencing diverse DNA-like polymers, including those with non-canonical nucleobases[67], expanding beyond the standard G, C, T, and A nucleobases used on Earth. This property is essential to allow agnostic nucleobase polymer sequencing for the study of life on Martian rocks. To make a definitive assessment of life's presence, this technique should be used alongside others, such as analysis of molecule-specific carbon, hydrogen and nitrogen isotopic ratios, analyses of molecular chirality, as well as the characterization of other polymers with life-related functions (like lipids from cell membranes). Finally, our analysis

of blanks within an ISO 5 cleanroom, highlights the importance of minimizing ambient and kitome contamination to prevent false positives. Maintaining ultra-cleanroom conditions and using DNA/RNA-free reagents at every stage of sample processing will be essential.

Methods

The sedimentary samples analysed in this work, listed in order of increasing age, are:

2800-year old microbialite from Alchichica Lake, Mexico. Alchichica Lake, an inland **saline lake** situated on the borders of Puebla, Tlaxcala, and Veracruz in the Central Mexican Plateau, serves as the study area[68]. The sampled microbialite originates from this lake (19°25′N, 97°24′W) at an elevation of 2305 meters above sea level. Alchichica is Mexico's deepest crater lake[68,69], with a maximum depth of 64 meters and an average depth of 39 meters[70,71]. The samples were collected on November 1, 2023. The lake's waters are primarily composed of NaCl and Na_2CO_3, classified as lacustrine evaporites, with a total dissolved solids concentration of 7235 mg/L[68]. Along its shoreline, microbialites are abundant. The analysed samples are dome-like microbialites, rich in hydromagnesite, huntite, and calcite. Their age, determined through $^{238}U/^{230}Th$ dating, is approximately ~2800 years[69,70]. Despite their initial formation dating back a few thousands of years, these microbialites, found near the shore within the lake, remain well-preserved and continue to support a diverse microbiome in the **shallow water of the lake**.

541 Ma stromatolites from the Anti-Atlas, Morocco. The stromatolite sample was collected at (30°39'54.36" N, 6°43'55.56" W), in the Anti-Atlas, in Morocco, on October 2, 2023. The carbonate stromatolite formation belongs to the Mançour Group of the Ouarzazate Supergroup; this location represents a significant geological formation from the Ediacaran period (about 635–541 Ma)[72,73]. The Mançour Group formation comprises volcanic, pyroclastic, and granitic rocks. These stromatolites (Conophyton) limestones outcrop over an area of 400 m by 500 m. The Mançour Group, part of the Ouarzazate Supergroup, was deposited in a volcanically influenced setting, suggesting that these stromatolites formed in **shallow marine environments** with volcanic and pyroclastic contributions. Individual stromatolites in such formations can vary in size, typically ranging from a few centimeters to several meters in height and diameter. The stromatolites primarily consist of carbonate minerals, likely limestone ($CaCO_3$) and dolomite ($CaMg(CO_3)_2$). Their formation is driven by microbial communities, primarily cyanobacteria, which trapped and bound sediments over time. Given the Ediacaran age, these structures are among the last stromatolites before the rapid diversification of animal life in the Cambrian.

~2930 Ma carbonate platform from the Red Lake area, Ontario, Canada. This is the oldest known preserved carbonate platform on Earth, with an estimated age of 2940 ± 2 Ma to 2925 ± 3 Ma[74]. Located within the Red Lake Greenstone Belt (RLGB) of the Uchi Subprovince in the western Superior Craton, this platform was deposited in an **open marine environment**. It represents a transgressive sequence, where rising sea levels progressively flooded the land, resulting in the deposition of different sedimentary facies[75]. The platform's stratigraphy consists of sedimentary rocks, predominantly dolomites (carbonate-rich) formed in **shallow** environments, interbedded with siltstone, sulfur-rich slates, and iron-rich formations deposited in **deeper environments**.

The selection of samples from this platform is based on two key factors. First, despite being the oldest known carbonate platform on Earth, its rocks remain relatively well-preserved. Second, it contains some of the earliest evidence of microbial life, preserved as stromatolites—sedimentary structures formed by cyanobacteria[76]. Early Martian and Terrestrial environmental conditions were likely similar, as extensively reviewed[77]. The diverse rock types and depositional environments of the Red Lake platform provide an excellent analogue for Martian geology, particularly for the Jezero crater. Carbonate rocks are rare on Mars, but Jezero crater is one of the few locations where carbonates have been identified along its shallow rim[78]. Additionally, iron-rich minerals have been described as primary components of the Jezero crater[78,79]. For this study, we selected:

1) **BL48 – Carbonate formation**. These samples were collected at (51°1'52" N, 94°13'15" W) on October 29th, 2021. The sample BL48 was collected from the BL12-37 drill core (from a depth of 133 m) in the Bridget Lake area, where it formed in the shallow part of the platform. Composed of dolomite ($CaMg(CO_3)_2$), it precipitated as the water became saturated with dissolved calcium and bicarbonate ions. This process was likely influenced by cyanobacteria, which perform photosynthesis, removing CO_2, increasing carbonate alkalinity and promoting the precipitation of carbonate minerals.
2) **NGI 1 - Oxide iron formation**. These samples were collected at (51°1'52" N, 94°11'36" W) on October 29th, 2021. The sample NGI 1 was collected from the NGI10-31 drill core (from a depth of 67.8 m) in the North Galena Island area and was formed in the deeper part of the platform. It is primarily composed of magnetite ($Fe^{2+}Fe^{3+}{}_2O_4$) interlaminated with chert (SiO_2). This sample was deposited when ferrous iron (Fe^{+2}) deeper, iron-rich waters reacted with slightly oxygenated waters near the redox boundary between the shallow carbonate shelf and the offshore lithofacies. This interaction led to the precipitation of ferric oxyhydroxides, which later transformed into magnetite during diagenesis[80].

Rock sample preparation. Samples were pulverized with a Fritsch Model "Pulverisette 2" mortar with an arm grinding speed of about 70 rpm. The mortar is composed of a base and a pestle that grinds by friction. This mortar is ideal for universal fine grinding from hard brittle to soft samples, as well as for preparing homogenised mixtures of grains. The final sample size obtained varies from 10 to 45 microns. The vials were sterilized at 550 °C for 12 h. Between 4 and 5 g per sample were put in borosilicate glass vials and sealed with a neutral atmosphere of N_2 (to mimic a neutral Martian atmosphere and avoid the production of reactive oxygen species and free radicals from the terrestrial atmosphere, which would cause additional damage). PTFE/silicone septa (20 mm magnetic crimp cap, 3 mm thick, Supelco) combined with aluminium crimp seals were used to seal the vials. While the exact leak rate of this configuration was not measured in this study, this sealing system is widely employed in chromatographic and trace gas analysis workflows, including volatile organic compound (VOC) sampling, where low permeability and high seal integrity are critical. Literature and manufacturer data support its suitability for short- to medium-term containment of analytes under ambient and controlled conditions.

Sample gamma irradiation and dose. Gamma (γ) photons are high-energy electromagnetic radiation with significant penetrating power that can indirectly ionize molecules by transferring energy to electrons in organic compounds, resulting in the formation of radicals and ions. We employed gamma-ray irradiation as a proxy for the ionizing cosmic and solar radiation that reaches Mars's surface. This method is commonly used in planetary environment simulations[43,44,57,58,63,81] due to its low cost and convenient setup.

The samples were sealed in a clear borosilicate glass vial with a 2 cm diameter and a wall thickness of $x = 0.13$ cm. The radiation attenuation from photons emitted by the radioactive source can be estimated using the Beer-Lambert equation. For gamma photons with energies between 0.1 and 20 MeV, the Mass Attenuation Coefficient (MAC) of borosilicate glass is 0.0240 cm^2/g[82]. With the density of borosilicate glass at $\rho = 2.23$ g/cm^3, we can calculate using the Beer-Lambert equation: $I = I_0\ exp\ (-\rho \cdot MAC \cdot x)$, resulting in $I = 0.9931\ I_0$. This indicates that the borosilicate glass vial wall absorbs only 0.69% of the applied dose.

1) **Irradiation dose D_1 (sterilization dose):** Radiation was applied to the sealed samples using gamma (γ) irradiation sources of Co^{60} (cobalt), which produces gamma rays with energies of 1.173 and 1.332 MeV.

The sterilization irradiation level D_1 was applied at ambient conditions during 12 days at the Universidad de Santiago de Compostela (Laboratorio de Radiofísica) to the microbialite samples, see Supplementary Fig. 1.

The ISO 11137-1 is the international standard that covers guidelines for sterilization using the radionuclide Cobalt-60 and Cesium-137, which are the two commonly used isotopes that emit gamma radiation. Given that some terrestrial organisms of the arctic have demonstrated resistance up to 0.1 MGy under Martian-like temperatures[83] we have increased the applied sterilization dose to 0.87 MGy. The incident radiation on the sample, after screening through the vial glass is $D_1 = 0.86$ MGy

2) **Irradiation dose D_2 (geological timescale dose):** The Martian-exposure geological scale **irradiation** level was applied to some samples at Centro de Investigaciones Energéticas, Medioambientales y Tecnológicas (CIEMAT) for 20 days at the National Facility for Irradiation of Materials (NAYADE). The samples were immersed in a sealed container in a water tank pool at ambient temperature. The net radiation rate inside the container was 21.91 kGy/h, and was previously calibrated by the NAYADE operators using three dosimeters and Fricke dosimetry.

Recent measurements, produced by RAD instrument on board Curiosity at Gale crater, suggest that the Galactic Cosmic Ray (GCR) radiation dose on the surface of Mars is of the order of 0.21 mGy/day[60], or equivalently 0.076 Gy/year. We have applied 10.52 MGy to the vials. The incident radiation on the sample, after screening through the vial glass is $D_2 = 10.45$ MGy. Based on the in situ measurements from RAD, this corresponds to 136 million years (where a Terrestrial year has 365 days).

Cleanroom analysis and controls. All the DNA extractions, dilutions, and library preparation for nucleobase sequencing were carried out inside a cleanroom environment of ISO (International Organization for Standardization) level 5[45]. Before any experimental setup, the working table, inside wall panels, and equipment were sprayed with 70% isopropyl alcohol and Chemgene HLD_4L and cleaned using the cleanroom sterile wipes. An ISO 5 Class cleanroom (class 100 cleanroom) is a semi-closed ultra-clean environment that utilises High Efficiently Particulate Air (HEPA) filtration systems to maintain air cleanliness levels of a maximum of 3520 particles (≥ 0.5 µm) per cubic meter of the inside air. There is an unavoidable background DNA introduced unintentionally during sample preparation, primarily from commercial reagents, mostly the DNA-extraction kits, or laboratory environments. These sequences can create false positives and misleading results. Nuclease-free water controls were used as blanks to quantify the level of contamination. All analyses were done in triplicate.

DNA extraction. Determining the minimum amount of degraded DNA fragments in rocks that can be sequenced with the current technology remains a significant challenge. Recent advances in nanopore sequencing allow for the analysis of DNA with only 2 pg, without amplification[84,85]. This technology can identify, and sequence reads as short as 20 nucleobases, with each nucleobase assigned a confidence level Q, indicating read quality.

Extracting DNA from soils and rocks, especially those with iron oxide, salts and other minerals, can be challenging due to factors like competitive binding and destructive chemical reactions. This is particularly critical for Martian analogue rocks[48,84,85]. To extract DNA from the pulverized rock samples, we have used the Qiagen DNeasy Powersoil Pro DNA kit (47014, Qiagen, UK) because it has been successfully used previously for the extraction of DNA from Mars Analogue Regolith powder MMS-2 and analogue soils[48,84,85], and Antarctic cryptoendoliths[86]. For each extraction, we aseptically transferred 0.5 g of the pulverized rocks, which was weighed directly into the Powerbead tubes. The tubes were then filled with 800 µl of the C1 lysis buffer and were briefly vortexed and incubated at 65 °C for 10 min. The Powerbead tubes were then vortexed at high speed for 5 min. The tubes were centrifuged at 15,000 g for 2 min, and 400–500 µl of the supernatant was carefully transferred to a centrifuge tube using sterile 100–200 µl filter tips for maximum recovery. Hereafter, the extraction procedure followed the manufacturer's instructions, and the final DNA was eluted in 40 µl of nuclease-free water (NEB, UK). As negative control for kitome contamination, 500 µl of nuclease-free water was DNA-extracted following the above procedure and eluted in 40 µl of fresh nuclease-free water.

DNA fluorescent mass quantification. DNA was quantified using a Qubit dsDNA 1X High Sensitivity (HS) assay kit for Qubit® 4.0 fluorometer (ThermoFisher Scientific®, UK), which has a lower limit of DNA detection of 5 pg/µl. Only a few samples had sufficient DNA mass to be detected with this method. DNA mass quantification was used to compare with the number of nucleobases sequenced with nanopore.

Nucleobase sequencing. Next Generation Sequencing technologies typically require ng to µg of input DNA. This limit impedes the microscale analysis of low biomass ecosystems and samples. Recent experiments have demonstrated the possibility of reducing this limit to pg (~100–1000 microbial cells) using Illumina[87], or nanopore technology[85]. At this extremely low level of biomass, the inclusion of negative controls to identify reagent-specific contaminants is recommended. DNA amplification is commonly used to overcome this difficulty, but this introduces considerable bias into metagenomic profiles. Here, we use nanopore sequencing without amplification.

The library for nanopore sequencing of all the samples was prepared using Ligation Sequencing Kit V14 (SQK-LSK114, Oxford Nanopore Technologies), which is compatible with their new chemistry R10.4.1 Flongle (FLO-FLG114) Flow Cells. The eluted DNA of each sample was directly used for the nanopore library preparation. The preparation steps were followed according to the manufacturer's instructions, except the volume for all the steps was halved as the samples were sequenced using a Flongle Flow Cell (R10.4.1) with a minimum of 50 or above active nanopores. Libraries for the above extracted nuclease-free water as a control were also prepared following the same procedure. ONT's Flongle Flow Cells require 125 µl priming mix and 30 µl gDNA library. At every library preparation stage, the specified reagents were transferred in an Eppendorf tube before adding the sample containing DNA to avoid losses due to pipetting. The bases were called for 20–24 h using MinKNOW version 24.02.6 with a lower limit Q-score of 1. The reads were analysed using FastQC (https://github.com/s-andrews/FastQC) and NanoQC (https://github.com/wdecoster/nanoQC) software compatible on Linux OS, in order to obtain GC content, total reads and nucleobases, mean read quality, and length. The library preparation protocol and sequence analysis were previously validated[85].

The output of the nanopore sequencing files also includes a quality score Q per read. The error probability can be calculated from a given quality score Q as $p=10^{-Q/10}$, i.e., a quality score of 10 represents a 1 in 10 chance of an incorrect base call (a base call accuracy of 90%), whereas a Q = 3 indicates a 50% error probability in the assignment of the base. The current version of the software is optimized for threads of at least 20 bases, but the base call accuracy is very low for threads shorter than 600 b.

Taxonomy annotation and reads length analysis. Nanopore raw reads FastQC files were concatenated by triplicates and quality control assessed with the software NanoComp v. 1.24.0 to create plots of length, quality and percent identity[88]. The Software SqueezeMeta v.1.6.3, specifically the sqm_reads.pl script, was used to perform the taxonomic and functional assignments of the reads[89]. Taxonomy annotation and reads abundance data obtained from SqueezeMeta program were imported in R statistics environment using the Metacoder (v0.3.7) package to produce the taxonomy trees[90,91]. The hits that were found in the blank were subtracted for this analysis.

Total Organic Carbon (TOC). For most of the samples, TOC was measured using isotope-ratio mass spectrometry (MAT 253 IRMS, Thermo Fisher Scientific), and following the analytical methods by the USGS[92]. The samples were homogenized using mortar and pestle. HCl (3 N) was added to the samples to remove carbonates, and, after equilibration for 24 h, adjusted to neutral pH with ultrapure water. The sample was oven dried (50 °C) until constant weight. Then, the content of total organic carbon (TOC %) was measured with an elemental analyser (HT Flash, Thermo Fisher Scientific), with two reference standards (Synthetic mixture soil-5 and Synthetic mixture soil-3, with 0.141 and 4.401% of TOC, respectively) from EuroVector SpA (Milan, Italy). The only exception to this was the measurement of TOC for the oxide iron formation sample, which was previously done using a different instrumental facility which can tolerate sulphur[46].

Linear and exponential fit. The fits were performed in Gnuplot software using the *nonlinear least-squares Marquardt-Levenberg algorithm*. This fit was applied to determine the radiolytic constant K and the linear correlation between total amount of nucleobases T and TOC in the pristine samples, and between T and the DNA mass in the microbialite samples. The linear fit of T to DNA mass is used to infer the mass for all other cases where the DNA concentration was below the Qubit detection limit. For this calculation we subtracted the number of bases (T) of the blank.

Data and materials availability

Sequence data are available at the European Nucleotide Archive (ENA) with open access project ID: PRJEB87056. All additional data are included in the Supplementary Information. Additionally, all sequencing data and data of the supporting information are accessible here https://github.com/FISABIO-BioinformaticsService/CommsEarth_Environment-fDNArocks.

Received: 15 April 2025; Accepted: 17 September 2025;
Published online: 24 October 2025

References

1. Tice, M. M. & Lowe, D. R. Photosynthetic microbial mats in the 3416-myr-old ocean. *Nature* **431**, 549–552 (2004).
2. Allwood, A. C. et al. Stromatolite reef from the Early Archaean Era of Australia. *Nature* **441**, 714–718 (2006).
3. Grotzinger, J. P. et al. A habitable fluvio-lacustrine environment at Yellowknife Bay, Gale Crater, Mars. *Science* **343**, 1242777 (2014).
4. Stern, J. C. et al. Organic carbon concentrations in 3.5-billion-year-old Lacustrine Mudstones of Mars. *Proc. Natl. Acad. Sci.* **119**, e2201139119 (2022).
5. Farley, K. A. et al. In situ radiometric and exposure age dating of the martian surface. *Science* **343**, 1247166 (2014).
6. Freissinet, C. et al. Organic molecules in the sheepbed mudstone, Gale Crater, Mars. *J. Geophys. Res.: Planets* **120**, 495–514 (2015).
7. Eigenbrode, J. L. et al. Organic matter preserved in 3-Billion-Year-Old mudstones at Gale Crater, Mars. *Science* **360**, 1096–1101 (2018).
8. Szopa, C. et al. First detections of dichlorobenzene isomers and trichloromethylpropane from organic matter indigenous to Mars mudstone in Gale Crater, Mars: results from the Sample Analysis at Mars Instrument onboard the Curiosity Rover. *Astrobiology* **20**, 292–306 (2020).
9. Millan, M. et al. Organic molecules revealed in Mars's Bagnold dunes by curiosity's derivatization experiment. *Nat. Astron.* **6**, 129–140 (2021).
10. Millan, M. et al. Sedimentary organics in Glen Torridon, Gale Crater, Mars: results from the SAM instrument suite and supporting laboratory analyses. *J. Geophys. Res. Planets* **127**, e2021JE007107 (2022).
11. Ming, D. W. et al. Volatile and organic compositions of sedimentary rocks in Yellowknife Bay, Gale Crater, Mars. *Science* **343**, 1245267 (2014).
12. Freissinet, C. et al. Long-chain alkanes preserved in a Martian Mudstone. *Proc. Natl. Acad. Sci. USA* **122**, e2420580122 (2025).
13. Kminek, G. et al. Mars sample return (MSR): planning for returned sample science. Astrobiology.Jun S-1-S-4. https://doi.org/10.1089/ast.2021.0198 (2022).
14. Hou, Z. et al. In search of signs of life on Mars with China's sample return mission Tianwen-3. *Nat. Astron* **9**, 783–792 (2025).
15. Farley, K. A. et al. Mars 2020 Mission Overview. Space Science Reviews, **216** https://doi.org/10.1007/s11214-020-00762-y (2020).
16. Farley, K. A. et al. Aqueously altered igneous rocks sampled on the floor of Jezero Crater, Mars. *Science* **377**, eabo2196 (2022).
17. Schon, S. C., Head, J. W. & Fassett, C. I. An overfilled lacustrine system and progradational delta in Jezero crater, Mars: implications for Noachian climate. *Planet. Space Sci.* **67**, 28–45 (2012).
18. Mangold, N. et al. Perseverance rover reveals an ancient delta-lake system and flood deposits at Jezero crater. *Mars. Sci.* **374**, 711–717 (2021).
19. Simon, J. I. et al. Samples collected from the floor of Jezero Crater With the Mars 2020 Perseverance Rover. *J. Geophys. Res. Planets* **128**, e2022JE007474 (2023).
20. Bosak, T. et al. Astrobiological potential of rocks acquired by the perseverance rover at a sedimentary fan front in Jezero Crater, Mars. *AGU Adv.* **5**, e2024AV001241 (2024).
21. Herd, C. R. et al. 'Sampling Mars: Geologic Context and Preliminary Characterization of Samples Collected by the NASA Mars 2020 Perseverance Rover Mission' PNAS, in print, (2024).
22. Sharma, S. et al. Diverse organic-mineral associations in Jezero Crater, Mars. *Nature* **619**, 724–732 (2023).
23. Scheller, E. L. et al. Aqueous alteration processes in Jezero Crater, Mars—implications for organic geochemistry. *Science* **378**, 1105–1110 (2022).
24. Scheller, E. L. et al. Inorganic interpretation of luminescent materials encountered by the Perseverance Rover on Mars. *Sci. Adv.* **10**, eadm8241 (2024).
25. Kminek, G. et al. COSPAR sample safety assessment framework (SSAF). *Astrobiology* **22**, S-186–S-216 (2022).
26. Glavin, D. P. et al. Abundant ammonia and nitrogen-rich soluble organic matter in samples from asteroid (101955) Bennu. *Nat. Astron.* **9**, 199–210 (2025).
27. Nie, P. et al. Synthetic life with alternative nucleic acids as genetic materials. *Molecules* **25**, 3483 (2020).
28. Wang, J. & Yu, H. Threose nucleic acid as a primitive genetic polymer and a contemporary molecular tool. *Bioorg. Chem.* **143**, 107049 (2024).
29. Kowalski, K. Synthesis and chemical transformations of glycol nucleic acid (GNA) nucleosides. *Bioorg. Chem.* **141**, 106921 (2023).
30. Nielsen, P. E. Peptide nucleic acids (PNA) in chemical biology and drug discovery. *Chem. Biodivers.* **7**, 786–804 (2010).
31. Kjær, K. H. et al. A 2-million-year-old ecosystem in Greenland uncovered by environmental DNA. *Nature* **612**, 283–291 (2022).
32. van der Valk et al. Million-year-old DNA sheds light on the genomic history of mammoths. *Nature* **591**, 265–269 (2021).
33. Killops, V. Killops Introduction to Organic Geochemistry (2nd ed.) (Blackwell Publishing, 2005).
34. Dabney, J., Meyer, M. & Pääbo, S. Ancient DNA damage. *Cold Spring Harb. Perspect. Biol.* **5**, a012567 (2013).
35. Martín-Torres, F. et al. Transient liquid water and water activity at Gale crater on Mars. *Nat. Geosci.* **8**, 357–361 (2015).
36. Zorzano, M.-P. et al. Present-day thermal and water activity environment of the mars sample return collection. *Sci. Rep.* **14**, 7175 (2024).

37. Clark, B. C. & Kounaves, S. P. Evidence for the distribution of perchlorates on Mars. *Int. J. Astrobiol.* **15**, 311–318 (2016).
38. Kounaves, S. P. et al. Identification of the perchlorate parent salts at the Phoenix Mars landing site and possible implications. *Icarus* **232**, 226–231 (2014).
39. Yen, A. S. et al. Evidence that the reactivity of the martian soil is due to superoxide ions. *Science* **289**, 1909–1912 (2000).
40. Lasne, J. et al. Oxidants at the surface of mars: a review in light of recent exploration results. *Astrobiology* **16**, 977–996 (2016).
41. Georgiou, C. D. et al. Radiation-driven formation of reactive oxygen species in oxychlorine-containing mars surface analogues. *Astrobiology* **17**, 319–336 (2017).
42. Pavlov, A. A. et al. Degradation of the organic molecules in the shallow subsurface of mars due to irradiation by cosmic rays. *Geophys. Res. Lett.* **39**, 2012GL052166 (2012).
43. Kminek, G. & Bada, J. The effect of ionizing radiation on the preservation of amino acids on Mars. *Earth Planet. Sci. Lett.* **245**, 1–5 (2006).
44. Ertem, G. et al. Evidence for the protection of n-heterocycles from gamma radiation by mars analogue minerals. *Icarus* **368**, 114540 (2021).
45. Mathanlal, T. et al. Design, Development, and operation of an ISO Class 5 cleanroom for planetary instrumentation and planetary protection protocols. *Heliyon* **10**, e36276 (2024).
46. Cañadas, F. et al. Archaean oxygen oases driven by pulses of enhanced phosphorus recycling in the ocean. *Nat. Geosci.* **18**, 430–435 (2025).
47. Suzuki, Y. et al. Subsurface microbial colonization at mineral-filled veins in 2-billion-year-old mafic rock from the Bushveld Igneous Complex, South Africa. *Microb. Ecol.* **87**, 116 (2024).
48. Xia, Z. et al. Deoxyribonucleic acid extraction from mars analog soils and their characterization with solid-state nanopores. *Astrobiology* **22**, 992–1008 (2022).
49. Hecht, M. H. et al. Detection of perchlorate and the soluble chemistry of martian soil at the phoenix lander site. *Science* **325**, 64–67 (2009).
50. Wadsworth, J. & Cockell, C. S. Perchlorates on Mars Enhance the Bacteriocidal Effects of UV Light. *Sci. Rep.* **7**, 4662 (2017).
51. Manrao, E. A. et al. Reading DNA at single-nucleotide resolution with a mutant mspa nanopore and phi29 DNA polymerase. *Nat. Biotechnol.* **30**, 349–353 (2012). (Crossref.
52. Clarke, J. et al. Continuous base identification for single-molecule nanopore DNA sequencing. *Nat. Nanotechnol.* **4**, 265–270 (2009).
53. Meutelet, R. et al. Extraction and purification of short DNA fragments from plasma using aqueous two-phase systems for liquid biopsy. *Sep. Purif. Technol.* **369**, 132884 (2025).
54. Maltais, T. R. et al. An Accounting of contamination control requirements, implementation, and verification of the sample tubes for the Mars 2020 mission and future return sample science. *Astrobiology* **23**, 846–861 (2023).
55. Yada, T. et al. Hayabusa-returned sample curation in the planetary material sample curation facility of JAXA. *Meteorit. Planet. Sci.* **49**, 135–153 (2014).
56. Tachibana, S. et al. Pebbles and Sand on Asteroid (162173) Ryugu: in situ observation and particles returned to Earth. *Science* **375**, 1011–1016 (2022).
57. Pavlov, A. A. et al. Rapid radiolytic degradation of amino acids in the martian shallow subsurface: implications for the search for extinct life. *Astrobiology* **22**, 1099–1115 (2022).
58. Pavlov, A. A., et al. Radiolytic effects on biological and abiotic amino acids in shallow subsurface ices on Europa and Enceladus. *Astrobiology* **24**, 698–709 (2024).
59. Sephton, M. A. et al. Thresholds of temperature and time for Mars sample return: final report of the Mars Sample Return Temperature-Time Tiger Team. *Astrobiology* **24**, 443–488 (2024).
60. Hassler, D. M. et al. Mars' surface radiation environment measured with the Mars Science Laboratory's Curiosity Rover. *Science* **343**, 1244797 (2014).
61. Cohen, B. A. et al. In situ geochronology on Mars and the development of future instrumentation. *Astrobiology* **19**, 1303–1314 (2019).
62. Quinn, R. C. et al. Perchlorate radiolysis on Mars and the origin of martian soil reactivity. *Astrobiology* **13**, 515–520 (2013).
63. Fox, A. C. et al. Radiolysis of macromolecular organic material in mars-relevant mineral matrices. *J. Geophys. Res. Planets* **124**, 3257–3266 (2019).
64. Couradeau, E. et al. Prokaryotic and Eukaryotic Community Structure in Field and Cultured Microbialites from the Alkaline Lake Alchichica (Mexico). PLoS ONE, edited by Jack Anthony Gilbert, 6, 2011, p. e28767. https://doi.org/10.1371/journal.pone.0028767.
65. Neveu, M. et al. The ladder of life detection. *Astrobiology* **18**, 1375–1402 (2018).
66. Green, J. et al. Call for a framework for reporting evidence for life beyond Earth. *Nature* **598**, 575–579 (2021).
67. Kawabe, H. et al. Enzymatic synthesis and nanopore sequencing of 12-letter supernumerary DNA. *Nat. Commun.* **14**, 6820 (2023).
68. Alcocer, J. Saline lake ecosystems of Mexico. *Aquat. Ecosyst. Health Manag.* **1**, 291–315 (1998).
69. Kaźmierczak, J., Kempe, S., López-García, P., Tavera, R. & Moreira, D. Modern and sub-recent carbonate microbialites from the alkaline crater lake Alchichica, Mexico. In J. Reitner, W. E. Krumbein, & G. Wörheide (Eds.), Geobiology of Stromatolites: International Kalkowsky-Symposium Göttingen (pp. 123–124) (Göttingen University Press, 2008).
70. Kaźmierczak, J. et al. Hydrochemistry and microbialites of the alkaline crater lake Alchichica, Mexico. *Facies* **57**, 543–570 (2011).
71. Arredondo-Figueroa, J. L., Borrego-Enriquez, L. E., Castillo-Dominguez, R. M. & Valladolid-Laredo, M. A. Batimetría y morfometría de los lagos "maars" de la cuenca de Oriental, Puebla. *México. Biótica* **9**, 23–39 (1983).
72. Thomas, R. J. et al. A new lithostratigraphic framework for the anti-atlas orogen, Morocco. *J. Afr. Earth Sci.* **39**, 217–226 (2004).
73. Gasquet, D. et al. Contribution to a geodynamic reconstruction of the anti-atlas (Morocco) during Pan-African Times with the emphasis on inversion tectonics and metallogenic activity at the Precambrian–Cambrian Transition. *Precambrian Res.* **140**, 157–182 (2005).
74. Corfu, F. & Wallace, H. U–Pb zircon ages for magmatism in the Red Lake Greenstone Belt, Northwestern Ontario. *Can. J. Earth Sci.* **23**, 27–42 (1986).
75. McIntyre, T. & Fralick, P. Sedimentology and geochemistry of the 2930 Ma Red Lake–Wallace Lake Carbonate Platform, Western Superior Province, Canada. *Depositional Rec.* **3**, 258–287 (2017).
76. Fralick, P. & Riding, R. Steep rock lake: sedimentology and geochemistry of an archean carbonate platform. *Earth-Sci. Rev.* **151**, 132–175 (2015).
77. Cabrol, N. A. The coevolution of life and environment on Mars: an ecosystem perspective on the robotic exploration of biosignatures. *Astrobiology* **18**, 1–27 (2018).
78. Horgan, B. H. N., Anderson, R. B., Dromart, G., Amador, E. S. & Rice, M. S. The mineral diversity of Jezero crater: evidence for possible lacustrine carbonates on Mars. *Icarus* **339**, 113526 (2020).
79. Schmidt, M. E. et al. Diverse and highly differentiated lava suite in Jezero Crater, Mars: constraints on intracrustal magmatism revealed by Mars 2020 PIXL. *Sci. Adv.* **11**, eadr2613 (2025).
80. Afroz, M. et al. Sedimentology and geochemistry of basinal lithofacies in the Mesoarchean (2.93 Ga) Red Lake Carbonate Platform, Northwest Ontario, Canada. *Precambrian Res.* **388**, 106996 (2023).
81. Bonner, W. A. et al. The radiolysis and radioracemization of amino acids on clays. *Orig. Life Evol. Biosph.* **15**, 103–114 (1985).

82. O. Kilicoglu, F. Akman, H. Ogul, O. Agar, U. Kara, Nuclear radiation shielding performance of borosilicate glasses: Numerical simulations and theoretical analyses, Radiation Physics and Chemistry, Volume 204, 110676, ISSN 0969-806X, (2023).
83. Cheptsov, V. S. et al. 100 kGy gamma-affected microbial communities within the ancient Arctic permafrost under simulated Martian conditions. *Extremophiles* **21**, 1057–1067 (2017).
84. Mojarro, A. et al. Nucleic acid extraction and sequencing from low-biomass synthetic mars analog soils for in situ life detection. *Astrobiology* **19**, 1139–1152 (2019).
85. Basapathi Raghavendra, J. et al. DNA sequencing at the picogram level to investigate life on Mars and Earth. *Sci. Rep.* **13**, 15277 (2023).
86. Maggiori, C. et al. Biosignature detection and MinION sequencing of antarctic cryptoendoliths after exposure to Mars simulation conditions. *Astrobiology* **24**, 44–60 (2024).
87. Rinke, C. et al. Validation of picogram- and femtogram-input DNA libraries for microscale metagenomics. *PeerJ* **4**, e2486 (2016).
88. De Coster, W. & Rademakers, R. NanoPack2: population-scale evaluation of long-read sequencing data. *Bioinformatics*, **39**, btad311 (2023).
89. Tamames, J. & Puente-Sánchez, F. SqueezeMeta, a highly portable, fully automatic metagenomic analysis pipeline. *Front. Microbiol.* **9**, 3349 (2019).
90. R. Core Team R: A Language and Environment for Statistical Computing. R Foundation for Statistical Computing, Vienna, Austria. https://www.R-project.org/ (Core Team, 2022).
91. Foster, Z. S., Sharpton, T. J. & Grünwald, N. J. Metacoder: an R package for visualization and manipulation of community taxonomic diversity data. *PLoS Comput Biol.* **13**, e1005404 (2017). PMID: 28222096; PMCID: PMC5340466.
92. Révész, K., Qi, H. & Coplen, T. B. Determination of the δ15N and δ13C of total nitrogen and carbon in solids. RSIL lab code 1832, chap. 5 of Stable isotope-ratio methods, sec. C of Révész, K. and Coplen, T.B. eds. Methods of the Reston Stable Isotope Laboratory (slightly revised from version 1.1 released in 2007): U.S. Geological Survey Techniques and Methods, book 10, 31 p., available only at https://pubs.usgs.gov/tm/2006/tm10c5/. (Supersedes versions 1.0 and 1.1 released in 2006 and 2007, respectively.) (USGS, 2012).

Acknowledgements

M.-P.Z. and D.C. were supported by grant PID2022-140180OB-C21 funded by MCIU/AEI /10.13039/501100011033/ FEDER, UE. QUADRAT NERC Doctoral Training Partnership, UKRI supported J.B.R. F.C. acknowledges support from MSCA grant agreement H2020-MSCA-IF-EF-ST/101022397. F.C. also acknowledges Dr. Philip Fralick (Lakehead University, Thunder Bay, Canada) for providing access to samples BL48 and NGI 1. J.M.-T. acknowledges the partial support of PID2023-146856NB-I00 funded by MICIU/AEI/10.13039/501100011033 and ERDF, EU, as well as support from the Alan and Norma Young Foundation and Oxford Nanopore Technologies. D.C. acknowledges the valuable support of Mohamed Beraaouz and Mohamed Hssaisoune during the field campaign in Morocco. We acknowledge Maria-Paz Martin Redondo for sample preparation. No permissions were required for sampling.

Author contributions

M.-P.Z. conceived the study, designed the research methodology, conducted radiation exposure tests, and wrote the original draft. J.B.R. extracted and sequenced DNA using nanopore technology in the cleanroom, analysing read length, quality, and GC content with FastQC and NanoQC, and DNA mass with Qubit. D.C. and F.C. performed TOC analysis, acquired the analogue samples, and offered expertise on their geological context and relevance as Mars analogue environments. M.R.-P. and G.D.A. analysed Fastq sequences for taxonomic classification, read length distribution, and phylogenetic tree construction. J.M.-T. provided expertise on Martian environmental conditions, as well as measurements from Curiosity rover, and facilitated access to the cleanroom and nanopore technology. All authors contributed to discussions, writing, and data analysis. M.-P.Z., D.C., F.C. and J.M.-T. secured funding.

Competing interests

The authors declare no competing interests.

Additional information

Supplementary information The online version contains supplementary material available at https://doi.org/10.1038/s43247-025-02809-w.

Correspondence and requests for materials should be addressed to Maria-Paz Zorzano.

Peer review information *Communications Earth & Environment* thanks Carol Stoker and Daniel Glavin for their contribution to the peer review of this work. Primary Handling Editors: Feifei Zhang and Joseph Aslin. A peer review file is available.